

Positively charged particles in dusty plasmas

A. A. Samarian,^{1,2} O. S. Vaulina,¹ A. P. Nefedov,¹ V. E. Fortov,¹ B. W. James,² and O. F. Petrov¹

¹*Institute for High Energy Densities, Russian Academy of Sciences, Moscow, 127412, Russia*

²*School of Physics, University of Sydney, NSW 2006, Australia*

(Received 3 January 2001; published 24 October 2001)

The trapping of dust particles has been observed in a dc abnormal glow discharge dominated by electron attachment. A dust cloud of several tens of positively charged particles was found to form in the anode sheath region. An analysis of the experimental conditions revealed that these particles were positively charged due to emission process, in contrast to most other experiments on the levitation of dust particles in gas-discharge plasmas where negatively charged particles are found. An estimate of the particle charge, taking into account the processes of photoelectron and secondary electron emission from the particle surface, is in agreement with the experimental measured values.

DOI: 10.1103/PhysRevE.64.056407

PACS number(s): 52.27.Lw, 52.25.Gj, 05.40.-a

I. INTRODUCTION

Dusty plasmas are low-temperature plasmas, consisting of neutral gas, ions, electrons, and micron-sized particles of solid matter (dust particles). These particles, which are immersed in the plasma, may acquire appreciable charges by collecting electrons and ions, and by emitting electrons [1,2]. When emission processes are unimportant, the equilibrium charge on the dust particles is negative as a result of the higher temperature and mobility of the electrons. The emission of electrons from the surface of a particle may, however, provide conditions for positive charging. Such differences in the sign of the charge on the dust particle can greatly modify the properties of plasma. In particular, in plasma with positive dust particles, the electron density would be larger than that of the ions, and instabilities and waves could be produced [3,4]. Also, the electron emission from the particles has been shown [5,6] to affect the electron Debye length, and thus, the condition for plasma crystal formation.

Because the positively charged dust occurs in the presence of strong ultraviolet (UV) radiation or fast electrons, plasmas with positive charged particles occur widely in space and also in the earth's mesosphere [7–9]. In order to understand how dusty plasmas are formed and how they affect various regions in space and in the earth's atmosphere, it is necessary to undertake laboratory investigations of positively charged dust systems. In laboratory conditions, the electrostatic force acting on the charged particles can compensate the gravity force resulting in levitation of the particles. At present, there is a large body of observations of levitated dust particles in capacitive rf discharges [10–15], inductive rf discharges [16,17], and dc glow discharges [18,19]. In these experiments, dust particles are observed in the form of distinct clouds at the edge of the plasma sheath, or near the electrode (for rf discharges) or, in the case of dc glow discharges, in the striation region and in artificially created electric double layers. All such experiments produce negatively charged particles.

Ordered, liquidlike structures of positive particles charged by thermionic emission have been observed in a laminar jet of thermal plasma [20], and under microgravity conditions where the charging was mainly due to photoemission [21]. A

common feature of these studies is the formation of weakly correlated structures of particles as they move in a dynamic stream. Steady-state conditions, as occur in gas discharge plasmas, are required to form ordered structures of positively charged particles. The absence of effective electrical traps capable of achieving levitation of positively charged particles has so far prevented any experimental observation of stable structures by these particles. Rosenberg discusses theoretically [6] a scheme for forming an ordered structure (Coulomb lattice) of positively charged particles. To the best of our knowledge, however, there have been no experimental observations of Coulomb structures consisting of positively charged dust particles in a laboratory plasmas.

In the present paper, the formation of an ordered structure of positively charged dust particles in the anode region of an abnormal dc glow discharge in air was observed. We estimate the charge on the particles, taking into account the processes of photoemission and secondary electron emission. The value of charge obtained agrees quite well with the results of probe measurements. Section II describes the experimental setup and observations. In Sec. III, we consider estimation of particle charge from probe measurements. In Sec. IV, we discuss the positive charging of dust particles due to secondary electron and photoelectron emission under conditions close to those of the experiment.

II. EXPERIMENT

In this experiment, the glow discharge is formed in a cylindrical stainless steel chamber with a specially shaped cold electrode (see Fig. 1). The chamber, with an inner diameter of 300 mm and height of 400 mm, has circular windows for illumination and observation. The cathode consists of two copper braces coupled by a molybdenum wire, and the anode is a metal foil disk; the electrode separation is 46 mm. The discharge current was varied from 0.5 to 15 mA, while the pressure of air was varied in the range 0.2–2 Torr. Measurements of plasma density, electron temperature, and strength of the electric field were obtained using single and quadruple tungsten cylindrical probes.

Thin-walled hollow spheres of borosilicate glass 10 μm in diameter were introduced into the plasma. The wall thickness

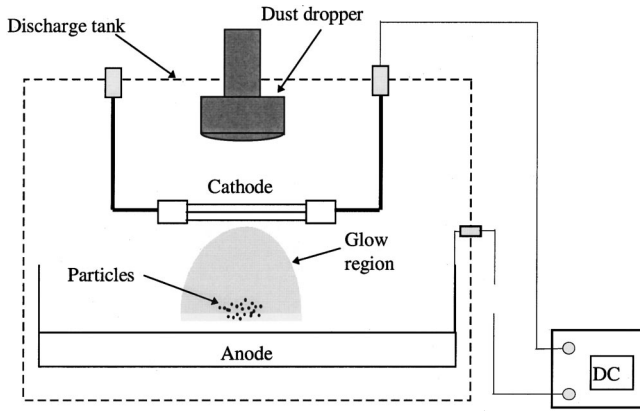
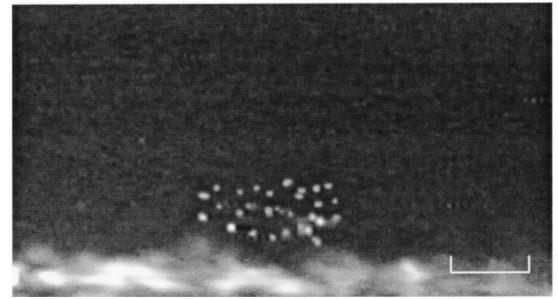


FIG. 1. Schematic diagram of the apparatus.

was approximately $2\text{--}3\ \mu\text{m}$ and the bulk particle density was close to $0.8\ \text{g/cm}^3$. A few grams of micron-sized particles were placed in a dust dropper located on the upper side of the tank. All the necessary observations were made by illuminating either horizontal or vertical planes with a sheet of Ar^+ (argon ion) laser light of thickness $250\ \mu\text{m}$ and breadth $20\ \text{mm}$. The height of the laser was adjustable. Scattered light was viewed through a window in the chamber. Individual particles could easily be seen with a charge-coupled device video camera fitted with a macro lens. Video images were recorded on tape recorder; frames were digitized with 720×540 resolution using an eight-bit monochrome frame grabber.

In our experiments, we observed the formation of a cloud consisting of several tens of particles several millimeters above the central part of the anode (see Fig. 2). After shaking the dust dropper, the dust particles fell past the equilibrium position, were reflected from the anode, and then became suspended at a certain point in space. In our experiment, we could not obtain a perfect crystal structure since, for any discharge parameters, the kinetic energy of the particles was more than $1\ \text{eV}$. Furthermore, the separation of the particles was not equidistant either within a layer nor between layers. The reason for not obtaining a perfect crystal structure might be that random charge fluctuations caused by the photoemission charging mechanism were relatively large [22], leading to heating of the dust particles [23,24]. As well, the particle temperature could be raised by the dispersive instability, which occurs in an inhomogeneous dusty plasma [25], producing spatial fluctuations of the grains similar to Brownian motion. The considerable spatial inhomogeneity may also explain the variation in particle separation.

When the discharge parameters were varied, the shape of the cloud and its position above the anode changed. For example, when the discharge current was reduced, the particle cloud rose and became elongated in the vertical direction. Figure 3(a) gives the effective cloud size $L = \sqrt{h^2 + l^2}$, where h is the vertical dimension of the cloud and l is its horizontal dimension, as a function of discharge current. Figure 3(b) shows how the distance H between the lower edge of the cloud and the anode varies as a function of the discharge current. The changing size and position of the cloud is a



a)



b)



c)

FIG. 2. Video images of the particle cloud at $P=0.3\ \text{Torr}$: for (a) $I=6.2\ \text{mA}$, (b) $3.8\ \text{mA}$, and (c) $10.8\ \text{mA}$. The scale in the figures corresponds to $5\ \text{mm}$.

result of changing plasma conditions. Figure 4 shows the variation of the relative intensity of emission and electron number density as function of the discharge current. Using this data, we estimate below the variation of particle charge. When the current approaches a critical value, which depends on pressure (for example, at $0.4\ \text{Torr}$ $I_{\text{cr}}=2.4\ \text{mA}$), the value of H increases sharply, i.e., at $I=I_{\text{cr}}$ the cloud “jumps away.” At a discharge current of $10\ \text{mA}$, we usually observed the formation of several clouds suspended low above the electrode [see Fig. 2(c)] and these merged into one as the discharge current decreased. It should be noted that the analysis of grain equilibrium positions in the anode region requires the development of a complete model including the calculation of the sheath parameters as function of the discharge current, which is beyond the scope of this paper. Instead, we concentrate on determining the value of the dust particle charge in the presence of emission processes.

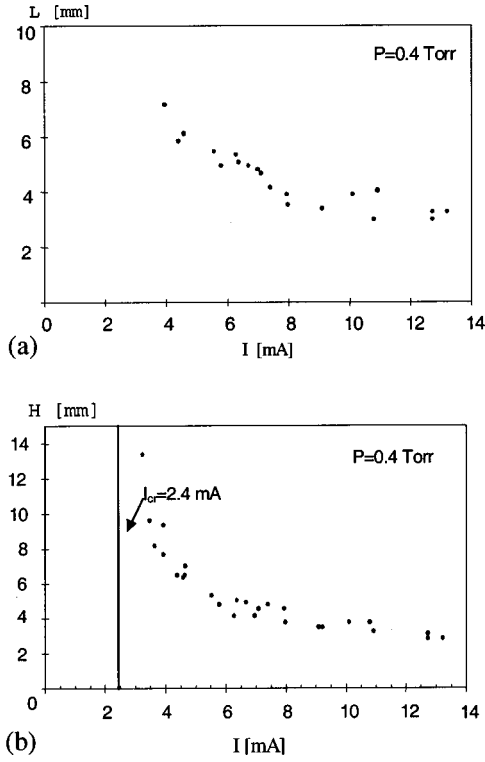


FIG. 3. Variation with discharge current of (a) the cloud dimension, L ; and (b) the distance between the particle cloud and the anode, H .

III. ESTIMATION OF DUST PARTICLE CHARGE

One of the basic problems of any dusty plasma experiment is determining the value and sign of the particle charge. The accuracy of particles charge measurement is, however, still an open question. There are many techniques used for charge measurement: the charge can be determined from resonant frequency measurements [26,27], dust-acoustic wave experiments [28,29], the analysis of horizontal collisions of dust particles pairs [30], the analysis of the trajectories of oscillating dust particles [31], dust sound speed measurements [32], and Mach cone experiments [33]. Most of these are, however, complicated, requiring special measurement procedures, and do not give precise results. On the other hand, for negatively charged particles, one can easily estimate the charge from probe measurements of plasma density and electron temperature [11,19,33,34]. For positively charged particles, such a simple estimation of charge is impossible because it is necessary to take into account the emission processes. In this paper, we obtain the charge value using another simple approach: the balance of forces acting on the particle in the vertical direction. After this paper was written, the authors learned of another paper [44] where the same approach was proposed for estimating the charge of particles levitated in an rf discharge sheath.

For a dust particle levitated in the sheath region, the following main forces act along the vertical z axis: the gravity force F_g , the electrostatic force F_{el} , the thermophoretic force F_{th} , and the ion drag force, F_i [35]. The total force acting on a particle at its equilibrium position is zero

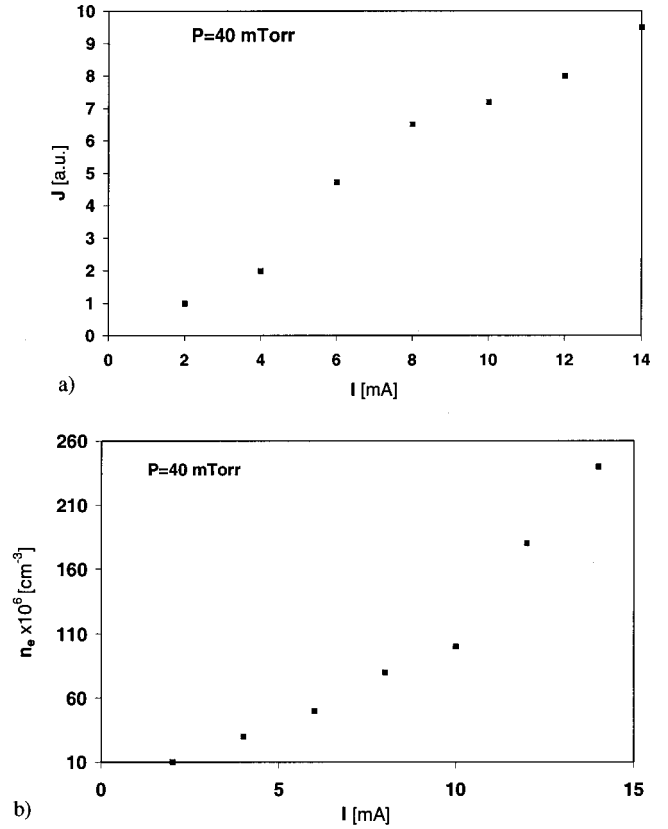


FIG. 4. Variation of (a) the relative intensity of discharge emission J and (b) the electron number density n_e as a function of discharge current I .

$$F_{el} - F_g + F_{th} + F_i = 0. \quad (1)$$

The negative sign before the gravity force indicates that this force acts downwards while all the other forces are acting upwards. The direction of the ion force is determined by the ion flux, the direction of the thermophoretic force by temperature gradient, and the direction of the electrostatic force by the sign of the anode fall.

Under our experimental conditions, it is impossible for a negative anode fall to exist for various reasons considered in [36]. Moreover, in our experiments $S_a < S_c \sqrt{m_e/m_i}$, where S_a and S_c are the anode and cathode areas, and m_e and m_i are the electron and ion masses, respectively. In Ref. [37], it has been shown that in such cases there should be a positive anode fall. This conclusion is confirmed by the observation of a narrow anode glow near the electrode. This suggests that the electrons are accelerated in the anode layer, acquiring energies ~ 15 – 30 eV, sufficient to excite air molecules. In addition, previous measurements and numerical estimates indicate that it is almost impossible for a negative anode fall to occur in an electronegative gas where the discharge is controlled by electron attachment [38].

As the ion flux and temperature gradient are directed away from the anode, the electrostatic, thermophoretic, and ion drag forces must compensate the gravity force to obtain levitation. Thus,

$$m_p g = eZ_d E + \frac{32}{15} \sqrt{\frac{\pi m}{8T}} a^2 \kappa \frac{\partial T}{\partial z} + \pi a^2 m_i n_i v_s^2 [\chi_1 + \chi_2], \quad (2)$$

where a , m_p , and Z_d are the particle radius, mass, and charge, respectively; T and m are the temperature and mass of the gas molecules, k is the thermal conductivity, $\partial T/\partial z$ is the temperature gradient, m_i is the ion mass, n_i is the concentration of positive ions, v_s is the velocity of ions in the sheath, χ_1 and χ_2 are given by

$$\chi_1 = 1 - \frac{2Z_d e^2}{m_i v_s^2 a}$$

$$\chi_2 = 2 \left(\frac{Z_d e^2}{m_i v_s^2 a} \right)^2 \ln \left(\frac{(\lambda_D/a)^2 + \left(\frac{Z_d e^2}{m_i v_s^2 a} \right)^2}{\left(1 - \frac{Z_d e^2}{m_i v_s^2 a} \right)^2} \right),$$

and λ_d is the screening length.

It is difficult to accurately determine the value of Z_d using Eq. (2) as it involves many parameters that cannot be measured exactly. However, we can simplify the problem if at first we use the experimentally obtained parameters to estimate the values of all forces. For the particles used, which have a radius $a = 5 \mu\text{m}$, the value of the gravity force F_g is $m_p g \approx 5 \times 10^{-12} \text{N}$. An estimate of the thermophoretic force gives $F_{\text{th}} < 10^{-14} \text{N}$, since the temperature gradient $\partial T/\partial z$ in the sheath does not exceed 5Kcm^{-1} . The upper limit of the ion drag force can be estimated, from simple formulas: $F_i < \pi a^2 n_i m_i v_i^2 (1 - eZ_d/amv_i^2)^2$, where $n_i \approx 10^8 \text{cm}^{-3}$, and v_i is the velocity of ions with energy $\sim 3 \text{eV}$. This gives $F < 10^{-18} \text{N}$ for the ion drag force; this estimate neglects, however, the fact that in an attachment-controlled discharge, a reverse propagating flux of negative ions having a concentration close to n_i will act in the opposite direction [38], further reducing the net ion drag force. Based on this reasoning, we can conclude that under the conditions of the present experiment, gravity may be compensated almost entirely by the electrostatic force F_{el} . Accordingly, Eq. (2) can be simplified to $m_p g = eZ_d E$ and the particle charge can easily be obtained from the following equation:

$$Z_d = \frac{m_p g}{eE}. \quad (3)$$

We obtain the value of the electric field using two different probe techniques. First, one can measure the electrode bias V_b and the plasma potential at the sheath boundary V_p , and then use the well-known approximation $V(z) = bz^2 + V_p$ for the potential variation in the sheath region [42], where z is the vertical coordinate. Thus, the electric field is given by

$$E(z) = E_0 - 2z(V_p - V_b)/h^2, \quad (4)$$

where E_0 is the value of electric field at electrode surface, and h is the thickness of the sheath. The second way is the direct measurement of the field using a quadruple probe [39].

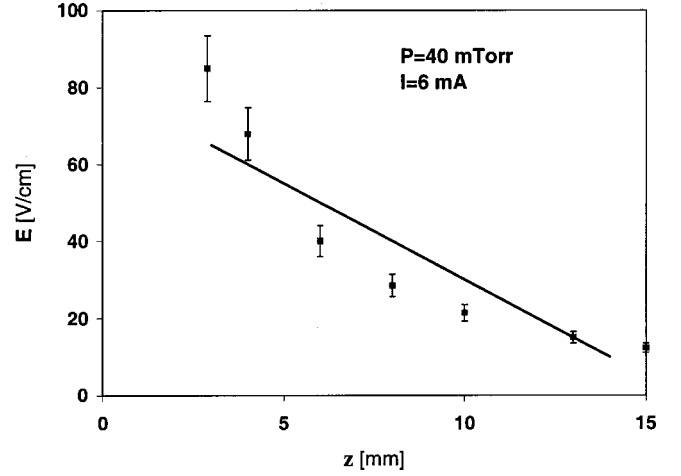


FIG. 5. Variation of electric-field E with distance from the electrode z . The solid line shows the results calculated from Eq. (4), and the points show E as measured by a quadruple probe.

Figure 5 shows that the results using both methods are in good agreement. Taking into account the value of the electric field $E^{\text{mean}} = 10\text{--}70 \text{V/cm}$ and the value of the gravitational force $m_p g \approx 5 \times 10^{-12} \text{N}$, we can conclude that the positive charge Z_d on a levitating particle of radius $a = 5 \mu\text{m}$ should be larger than 1500 elementary charges (i.e., $Z_d > 1.5 \times 10^3$). In the next section, we estimate the value of particle charge using a theoretical approach.

IV. ANALYSIS OF DUST PARTICLE CHARGING

The charge on a dust particle is the result of the net affect of all possible currents to the particle surface. Thus, the equilibrium charge Z_d is found from the condition for zero current

$$I(Z_d) = I_{\text{em}} + I_{\text{pl}} = 0, \quad (5)$$

where I_{em} is the current due to emission processes, and I_{pl} is current due to election and ion fluxes. In normal glow discharges, where the emission processes are insignificant, the main charging mechanism is absorption of plasma electrons and ions by the particle. As a result the dust particles become negatively charged [2,40]. In electronegative gas discharges controlled by electron attachment, the number density of the positive and negative ions have similar values, and the electron density may be one or two orders of magnitude lower than the ion densities [42]. Because of the large difference between the ion and electron mass, and taking into account the higher temperature of the latter, the dust particles cannot acquire net positive charge without electron emission from their surface. Electron emission constitutes a positive current to the particle, and it can lead to the particle becoming positively charged. In our paper, we assume that the dust particles acquire a positive charge due to photoelectric and secondary electron emission. These emission mechanisms are the most important for laboratory dusty plasma in gas dis-

charges, and their joint actions are able to compensate for the thermal electron flux onto a dust particle from the bulk plasma.

A gas discharge plasma is a source of UV radiation due to electron-impact excitation of neutrals. However, this radiation is usually too weak to alter the dust charge significantly in either normal dc discharges or rf discharges. The discharge under study has parameters similar to those of an abnormal hollow cathode discharge, the main characteristics being a strong electric field in the cathode space and an electron density maximum at the center of the discharge [41]. This leads to an increase of the power of the UV radiation from the cathode region. Another characteristic of this type of discharge is the non-Maxwellian electron energy distribution function due to the presence of a great number of high-energy ($U_o > 50$ eV) electrons. These characteristics suggest the existence of effective mechanisms for particle charging by photoelectric and secondary electron emissions. Below, we consider the effect of these mechanism on dust particle charge for conditions close to those of the experiment.

A. Plasma electron current

The electron (ion) current to the dust particle surface from the surrounding plasma is given by orbit motion limited theory [22,40] when $a \ll \lambda_d \ll \lambda_{mfp}$, where λ_{mfp} is a mean free path for electron-neutral or ion-neutral collisions. Taking into account the mass of ions with respect to the electron mass, and the fact that the ions are close to room temperature, we may neglect the currents of the positive and negative ions compared to that of the electrons. Generally, the electron current I_e onto the dust particle surface is a complicated function of the thermal velocity $v_T = (2kT_e/m_e)^{1/2}$, where T_e is the electron temperature, and the drift velocity $v = (2U_o/m_e)^{1/2}$, where U_o is the kinetic energy of drift electrons [2]. For simplicity, we consider two types of electrons in the anode region of an abnormal dc discharge: thermal electrons with number density n_e , characterized by temperature T_e , and high-energy electrons with number density n_e^h , and kinetic-energy $U_o \gg kT_e$. For Maxwellian electrons, the orbit-limited current to an attracting isolated spherical particle with an equilibrium surface potential $\phi_s > 0$ relative to the surrounding plasma is

$$I_T = 4\pi a^2 e n_e (2kT_e/m_e)^{1/2} (1 + e\phi_s/kT_e). \quad (6)$$

In the case of the monoenergetic fast electrons, we have

$$I_h = \pi a^2 e n_h (2U_o/m_e)^{1/2} (1 + e\phi_s/U_o). \quad (7)$$

B. Secondary electron current

Assuming a Maxwellian distribution with temperature T_s for the secondary-emission electrons, the secondary-emission current I_{se} from an isolated spherical particle ($\phi_s > 0$) is given by

$$I_{se} = \delta I_h (1 + e\phi_s/kT_s) \exp(-e\phi_s/kT_s), \quad (8)$$

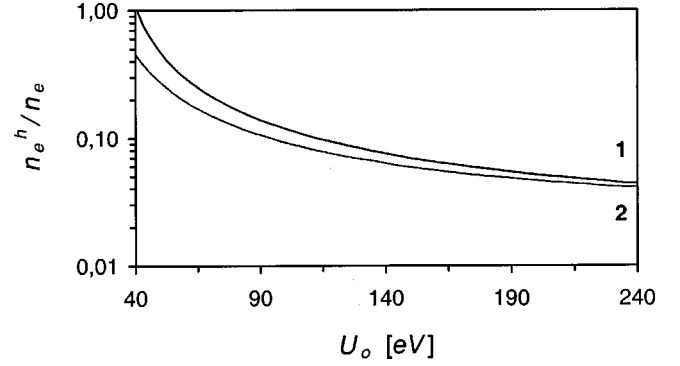


FIG. 6. Dependency of the ratio of number densities $n_e^h/n_e(\phi_s = 0)$ on the energy U_o of the fast electrons $\phi_s = 0$ for glass with $\delta_m = 3$ and different U_m : 1 – $U_m = 300$ eV; 2 – $U_m = 400$ eV.

where δ is the secondary-emission coefficient. For bulk materials, the energy dependence of δ is [40]

$$\begin{aligned} \delta(U_m, \delta_m, U) = & 7.4\delta_m(U_o + e\phi_s) \\ & \times \exp(-2\{(U_o + e\phi_s)/U_m\}^{1/2})/U_m, \end{aligned} \quad (9)$$

where U_m and δ_m are material constants. Different types of glasses, for example, have $\delta_m = 2-4$ for energies $U_m = 200-400$ eV [40,42]. Typical values of T_s are from 1–5 eV.

If we assume a Fermi distribution for the secondary-emission electrons, the secondary-emission current I_{se}^* from a positively charged spherical particle is given by [1]

$$\begin{aligned} I_{se}^* = & \delta I_h [e\phi_s/kT_s \ln\{1 + \exp(-e\phi_s/kT_s)\} \\ & + \Phi(-e\phi_s/kT_s)] / \Phi(E_F/kT_s), \end{aligned} \quad (10)$$

where E_F is the Fermi energy, and $\Phi(\chi) = \int_0^{\exp(\chi)} \Omega \ln(1 + \Omega) d\Omega$ is a well-known tabulated function. Typical values of E_F for different types of glasses are in the range 0.05–0.5 eV [43]. Because of this the E_F/kT_s value for glasses is small, and $\Phi(E_F/kT_s) \rightarrow \pi^2/12$.

In the case of a dust cloud, which is transparent to the emitted electrons, the equilibrium particle surface potential ϕ_s can be found from Eqs. (6)–(8) by equating $I_T + I_h$ and I_{se} [or I_{se}^* (10)]. The sign of the charge on the dust will vary with the value of the ratio of number densities n_e^h/n_e . The n_e^h/n_e value, which leads to $\phi_s = 0$, is shown in Fig. 6 for different energies U_o of the fast electrons for glass with $\delta_m = 3$ ($I_{se}^* \approx I_{se}$). Large values of n_e^h/n_e will produce positive charging of the dust; small values will lead to negative charging. The dependency of the equilibrium particle potential ϕ_s on the ratio n_e^h/n_e is shown in Fig. 7 for different values U_o .

C. Photoemission current

We consider a monochromatic UV source with a unidirectional flux of photons of energy $h\nu \approx 8.2$ eV, corresponding to the UV resonance line of nitrogen. Assuming a Max-

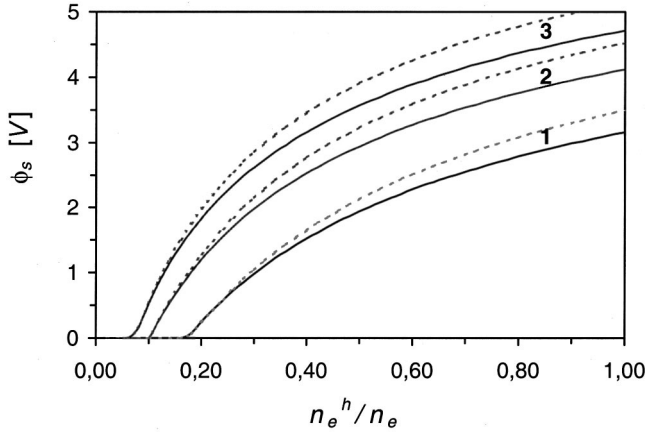


FIG. 7. Dependency of the equilibrium potential ϕ_s on the ratio n_e^h/n_e for different values of the energy U_0 : 1–60 eV; 2–90 eV; 3–120 eV. (solid lines, Maxwellian distribution; dashed lines, Fermi distribution).

wellian distribution with temperature T_{ph} for the emitted photoelectrons, the photoemission current I_{ph} from an isolated spherical particle ($\phi_s > 0$) is given by

$$I_{ph} = \pi a^2 e Q_{abs} Y J (1 + e \phi_s / k T_{ph}) \exp([\xi - e \phi_s] / k T_{ph}). \quad (11)$$

Here, Q_{abs} is the efficiency of absorption of the UV radiation ($Q_{abs} \approx 1$ for $2\pi a/\lambda \gg 1$, where λ is the wavelength [6,22]), J is the photon flux, Y is the photoelectric efficiency, and $\xi = h\nu - W$, where $h\nu$ is the photon energy, and W is the photoelectric work function. Typical values of W for different materials are in the range 1–6 eV; for example, glasses have $W = 4.0$ –5.2 eV. The values of Y depend on the photon energy $h\nu$. For $h\nu > 7$ –8 eV, the photoelectric efficiency varies from 0.1 to 1 for metals, and from 0.01 to 0.1 for dielectrics (for glasses $Y \approx 0.1$). Typical values of T_{ph} are in the range 1–2 eV.

If a Fermi distribution is assumed for the emitted photoelectrons, the photoemission current I_{ph}^* from a positively charged spherical particle is given by [1]

$$I_{ph}^* = \pi a^2 e Q_{abs} Y J [e \phi_s \ln\{1 + \exp(\chi)\} / k T_{ph} + \Phi(\chi)] / \Phi(E_F / k T_{ph}), \quad (12)$$

where $\chi = (\xi - e \phi_s) / k T_{ph}$.

For a unidirectional photon flux with $h\nu > W$, the photoemission current I_{ph}^{**} is usually approximated as [6,40]

$$I_{ph}^{**} = \pi a^2 e Q_{abs} Y^{**} J \exp(-e \phi_s / k T_{ph}), \quad (13)$$

where Y^{**} is an effective value (the yield of the photoelectrons) close to 1 for metals, and to 0.1 for dielectrics. This approach is attractive when the characteristics of the particle material (W), or radiation flux ($h\nu$) are not well known.

Assuming a dust cloud that is transparent for the emitted photoelectrons, the equilibrium particle surface potential ϕ_s can be found from Eqs. (6), (11)–(13) by equating I_T , and I_{ph} (I_{ph}^* , I_{ph}^{**}). For the different approaches (11)–(13), the

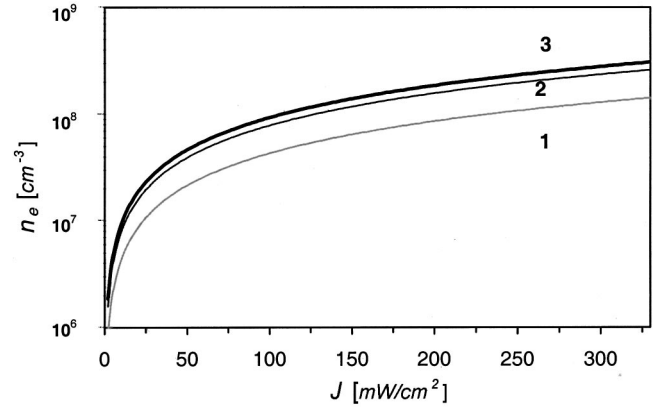


FIG. 8. Dependency of the number density n_e of the electron current I_T on the photon flux J in the case of $\phi_s = 0$ for glass with $Y \equiv Y^{**} = 0.1$, $W = 5$ eV, and $h\nu = 8.2$ eV, for the following cases: 1, Fermi distribution; 2, Maxwellian distribution; 3, approximation (13).

dependency of the number density n_e of the electrons in the current I_T on the photon flux J that leads to $\phi_s = 0$ is shown in Fig. 8 for glasses with $Y \equiv Y^{**} = 0.1$, $W = 5$ eV and $h\nu = 8.2$ eV. The resulting dependency of the equilibrium particle potential ϕ_s on the photon flux J for $n_e = 10^7$ cm $^{-3}$ is shown in Fig. 9 as bold lines.

Figure 9 also illustrates the effect on the variation of equilibrium potential ϕ_s with photon flux when secondary electron emission is included. In this case, the equilibrium potential ϕ_s of the positively charged dust particles was obtained from

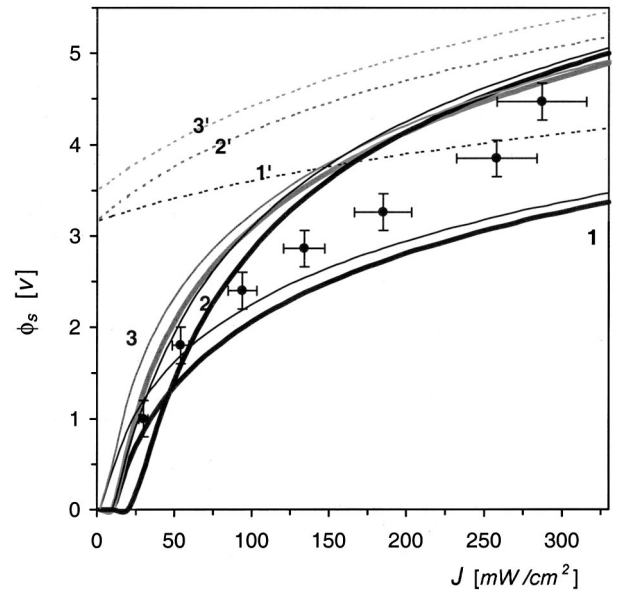


FIG. 9. Dependency of the equilibrium particle potential ϕ_s on the photon flux J for the number density $n_e = 10^7$ cm $^{-3}$ and for the following cases: 1, approximation (10); 2, Fermi distribution; 3, Maxwellian distribution, under different conditions of particle charging: photoemission with $n_e^h/n_e = 0$ (bold lines); photo and secondary electron emissions with $n_e^h/n_e = 0.1$ (fine solid lines), and $n_e^h/n_e = 1$ (dashed lines). The points represent the experimentally measured ϕ_s .

$$I_T + I_h = I_{se}(I_{se}^*) + I_{ph}(I_{ph}^*) \quad (14a)$$

for Maxwellian (Fermi) approximations, and from

$$I_T + I_h = I_{se} + I_{ph}^{**} \quad (14b)$$

for approach (13). The significance of the contribution of the secondary electron emission is determined by the number density ratio (n_e^h/n_e). It can be seen that for $n_e^h/n_e \leq 0.1$ photoemission provides the main contribution to particle charging.

The particle surface potential ϕ_s can also be estimated from the experimentally measured particle charge from the relationship $\phi_s \approx eZ_d/a$. These results are also shown in Fig. 9 for $a = 5 \mu\text{m}$, taking into the account that J is directly proportional to the discharge current (see Fig. 4), and that the photon flux J was equal to 0.03 W/cm^2 for a current of 2.6 mA. Comparing the calculated and experimental results, we conclude that the values obtained for particle surface potential are in good agreement with our analytical estimates. Notice that the measured values suggest that under our experimental conditions, the role of secondary electron emission is insignificant and that the charging of dust particles is predominantly by photoemission. In spite of this, the uncertainty of the value of n_e^h/n_e did not allow us to determine which from among the Fermi distribution, the Maxwellian distribution, or approximation (12) is best able to describe the photoemission charging of dust particles.

V. CONCLUSIONS

In the present study, levitation of positively charged dust particles in the anode region of a dc glow discharge has been observed experimentally. A dust cloud consisting of several tens of particles formed above the central region of the anode. By varying the discharge parameters, it was possible to change the shape of the cloud and control its position above the anode.

An analysis of the experimental conditions shows that the charge of the levitating particles is positive, which significantly distinguishes this experiment from most discharge experiments where the dust particles are negatively charged. Our results show that under our experimental conditions, the role of secondary electron emission is insignificant with the charge on the dust particles predominantly due to photoemission. An estimate of the charge agrees with the results of measurements of the electric field, which is required for dust particle levitation in the earth's gravitational field.

ACKNOWLEDGMENTS

The authors thank Dr. A. V. Chernyshev and Mr. A. M. Lipaev for assistance with the experiments. This work was supported by the Australian Research Council, Science Foundation for Physics within the University of Sydney and the Russian Fund for Basic Research, Grant No. 81-01-1665.

-
- [1] M. S. Sodha and S. Guha, *Adv. Plasma Phys.* **4**, 219 (1971).
 - [2] E. C. Whipple, *Rep. Prog. Phys.* **44**, 1197 (1981).
 - [3] K. N. Ostrikov, M. Y. Yu, and L. Stenflo, *Phys. Rev. E* **61**, 782 (2000).
 - [4] S. I. Popel, A. A. Gisko, A. P. Golub', T. V. Losseva, R. Bingham, and P. K. Shukla, *Phys. Plasmas* **7**, 2410 (2000).
 - [5] M. Rosenberg and D. A. Mendis, *IEEE Trans. Plasma Sci.* **23**, 177 (1995).
 - [6] M. Rosenberg, D. A. Mendis, and D. P. Sheehan, *IEEE Trans. Plasma Sci.* **24**, 1422 (1996).
 - [7] T. Nitter, O. Havnes, and F. Melandso, *J. Geophys. Res.* **103**, 6605 (1998).
 - [8] E. Grun, G. E. Morfill, and D. A. Mendis, in *Planetary Rings*, edited by Brahic and Greenberg (University Arizona Press, Tucson, 1984).
 - [9] O. Havnes *et al.*, *J. Geophys. Res.* **101**, 10 839 (1996).
 - [10] J. H. Chu and I. Lin, *Phys. Rev. Lett.* **72**, 4009 (1994).
 - [11] H. Thomas *et al.*, *Phys. Rev. Lett.* **73**, 652 (1994).
 - [12] Y. Hayashi and K. Tachibana, *Jpn. J. Appl. Phys., Part 2* **33**, L804 (1994).
 - [13] A. Melzer, T. Trottenberg, and A. Piel, *Phys. Lett. A* **191**, 301 (1994).
 - [14] G. Praburam and J. Goree, *Phys. Plasmas* **3**, 1212 (1996).
 - [15] S. Nunomura, N. Ohno, and S. Takamura, *Phys. Plasmas* **5**, 3517 (1998).
 - [16] Yu. V. Gerasimov *et al.*, *Tech. Phys. Lett.* **24**, 774 (1998).
 - [17] H. H. Hwang, E. R. Keiter, and M. J. Kushner, *J. Vac. Sci. Technol. A* **16**, 2454 (1998).
 - [18] V. E. Fortov *et al.*, *Phys. Lett. A* **229**, (1997).
 - [19] A. M. Lipaev *et al.*, *JETP Lett.* **85**, 1110 (1997).
 - [20] V. E. Fortov *et al.*, *Phys. Lett. A* **219**, 89 (1996).
 - [21] V. E. Fortov *et al.*, *JETP Lett.* **87**, 1087 (1998).
 - [22] S. A. Khrapak, O. S. Vaulina, A. P. Nefedov, and O. F. Petrov, *Phys. Rev. E* **59**, 6017 (1999).
 - [23] O. S. Vaulina, S. A. Khrapak, O. F. Petrov, and A. P. Nefedov, *Phys. Rev. E* **60**, 5959 (1999).
 - [24] R. A. Quinn and J. Goree, *Phys. Rev. E* **61**, 3033 (2000).
 - [25] O. S. Vaulina, A. P. Nefedov, O. F. Petrov, and V. E. Fortov, *JETP Lett.* (to be published).
 - [26] T. Trottenberg, A. Melzer, and A. Piel, *Plasma Sources Sci. Technol.* **4**, 450 (1995).
 - [27] A. Homann, A. Melzer, and A. Piel, *Phys. Rev. E* **59**, R3835 (1999).
 - [28] J. B. Pieper and J. Goree, *Phys. Rev. Lett.* **77**, 3137 (1996).
 - [29] A. A. Samarian, A. V. Chernyshev, A. P. Nefedov, O. F. Petrov, and V. Fortov, *JETP* **92**, 454 (2001).
 - [30] U. Konopka, L. Ratke, and H. Thomas, *Phys. Rev. Lett.* **79**, 1269 (1997).
 - [31] E. B. Tomme, B. M. Anaratone, and J. E. Allen, *Plasma Sources Sci. Technol.* **9**, 87 (2000).
 - [32] S. Nunomura, D. Samsonov, and J. Goree, *Phys. Rev. Lett.* **84**, 5141 (2000).
 - [33] D. Samsonov, J. Goree, Z. W. Ma, A. Bhattacharjee, H. M. Thomas, and G. E. Morfill, *Phys. Rev. Lett.* **83**, 3649 (1999).
 - [34] S. Nunomura, T. Misawa, N. Ohno, and S. Takamura, *Phys. Rev. Lett.* **83**, 1970 (1999).

- [35] T. Nitter, *Plasma Sources Sci. Technol.* **5**, 93 (1996).
- [36] V. L. Granovsky, *Electric Current in a Gas* (Nauka, Moscow, 1971).
- [37] V. Nikulin, *J. Tech. Phys.* **81**, 356 (1987).
- [38] Yu. P. Rayzer, M. N. Shneyder, and N. A. Yatsenko, *High-Frequency Capacitive Discharge* (Nauka, Moscow, 1995).
- [39] N. P. Ovchinnikova *et al.*, *Prib. Tekh. Eksp.* **45**, 456 (1992).
- [40] J. Goree, *Plasma Sources Sci. Technol.* **3**, 400 (1994).
- [41] B. I. Moskalev, *Discharge with Hollow Cathode* (Energiya, Moscow, 1969).
- [42] Yu. P. Rayzer, *Physic of Gas Discharge* (Nauka, Moscow, 1987).
- [43] G. V. Samsonov, *Physical-Chemical Characteristics of Oxides* (Metallurgiya, Moscow, 1978).
- [44] E. B. Tomme, D. A. Law, B. M. Annaratone, and J. E. Allen, *Phys. Rev. Lett.* **85**, 2518 (2000).